Crystallography Reports, Vol. 43, No. 4, 1998, pp. 631–639. Translated from Kristallografiya, Vol. 43, No. 4, 1998, pp. 680–688.

Defect Density Waves and Specific Manifestations of the Memory Effect in Crystals with Incommensurate Phases

I. M. Shmyt'ko and B. Sh. Bagautdinov

Institute of Solid-State Physics, Russian Academy of Sciences, Chernogolovka, Moscow oblast, 142432 Russia

Received August 9, 1996

Abstract—The X-ray diffraction studies of $SC(NH_2)_2$, TMA–$ZnCl_4$, and Ag_3AsS_3 crystals revealed specific manifestations of the memory effect associated with defect density waves: the appearance of additional modulation waves and their interactions with the ordinary wave, an increase of the temperature range corresponding to the incommensurate phase, the superposition of several modulated phases, and the reverse temperature hysteresis characterizing the transition from the normal to the incommensurate one phase.

Many crystals with incommensurate phases exhibit the memory effects that manifest themselves as temperature anomalies in their physical properties when observed after a prolonged exposure at a constant temperature T_0 chosen within the incommensurability range [1–5]. Some researchers attribute these effects to the interaction of the structural modulations with the mobile lattice defects. It is assumed that, as the sample is kept at the above-mentioned constant temperature, this interaction causes the rearrangement of defects, and their density becomes modulated with the period equal to that of the initial structure at this temperature. The rearrangement stems from the lowering of the defect activation energy down to 0.1 eV in the small displacement range [6] of the incommensurate wave. The lowering of the activation energy gives rise to a significant growth of the defect concentration in the interstitial sites of the modulated lattice. The defects become concentrated between the nodes of the wave, and, therefore, they form a defect density wave (DDW) with the period coinciding with that of the modulation wave at the annealing temperature.

When the crystal temperature approaches T_0 for the second time, the defect density wave "captures" the structural modulation thus revealing the memory of the previous events and giving rise to the plateau in the temperature dependences of a number of different physical parameters. In addition, the defect density waves result in specific structural states that were not observed in the crystals without DDW. In this paper we present the X-ray diffraction patterns testifying to the existence of DDW and analyze the effect of DDW on the structural states of certain crystals.

We studied the $SC(NH_2)_2$ (thiourea), TMA–$ZnCl_4$, and Ag_3AsS_3 (proustite) crystals. In thiourea, the modulated structure arises within the 202–169 K temperature range intermediate between the paraelectric (*Pnma*) and ferroelectric ($P2_1ma$) phases. The structure of the incommensurate phase is characterized by the rotation of $SC(NH_2)_2$ molecules about the *b*-axis with wave vector $\mathbf{q} = \delta\mathbf{b}^*$ (δ = 1/7–1/9), where δ is the parameter of incommensurability and $\mathbf{b}^*$ is the reciprocal lattice vector of the generic phase.

In TMA–$ZnCl_4$ under the atmospheric pressure, there are five structural transformations: *Pmcn* (incommensurate)–$P2_1cn$–$P112_1/n$–$P12_1/c1$–$P2_12_12_1$ at 23, 7, 3.4, –91, and –112°C, respectively, The modulations in the incommensurate phase are characterized by the wave vector $\mathbf{q} = (2/5 + \delta)\mathbf{c}^*$. In the polar phase, ($P2_1cn$), the lattice constant *c* is by a factor of five greater than in the initial structure ($\mathbf{q} = 2/5\mathbf{c}^*$). In the ferroelastic phase ($P112_1/n$), the lattice period is tripled along the **c** axis ($\mathbf{q} = 1/3\mathbf{c}^*$). The temperature range corresponding to the polar phase shrinks under effect of the oriented stresses normal to the polar axis. When the stresses attain the critical value $\sigma_{yy} \cong 40$ bar, the polar phase disappears.

Proustite in the normal state belongs to the $R3c$ space group. At 60 K, it transforms to an incommensurably modulated phase with the modulation wave vectors along the $(hkl) \pm 1/3\{(1–1.0), \pm(01.1), \pm(–10.1)\}$ direction. At 50 K, it undergoes a lock-in transition to a commensurate phase with the tripled lattice parameter. The three-dimensional space group characterizing the symmetry of the modulated phases coincides with the symmetry group of the normal phase. Below 28–30 K, the symmetry of the Ag_3AsS_3 crystal reduces to the triclinic system, and the crystal becomes ferroelectric with no multiplication of the initial structure periods [7].

1063-7745/98/4304-0631$15.00 © 1998 МАИК Наука / Interperiodica Publishing

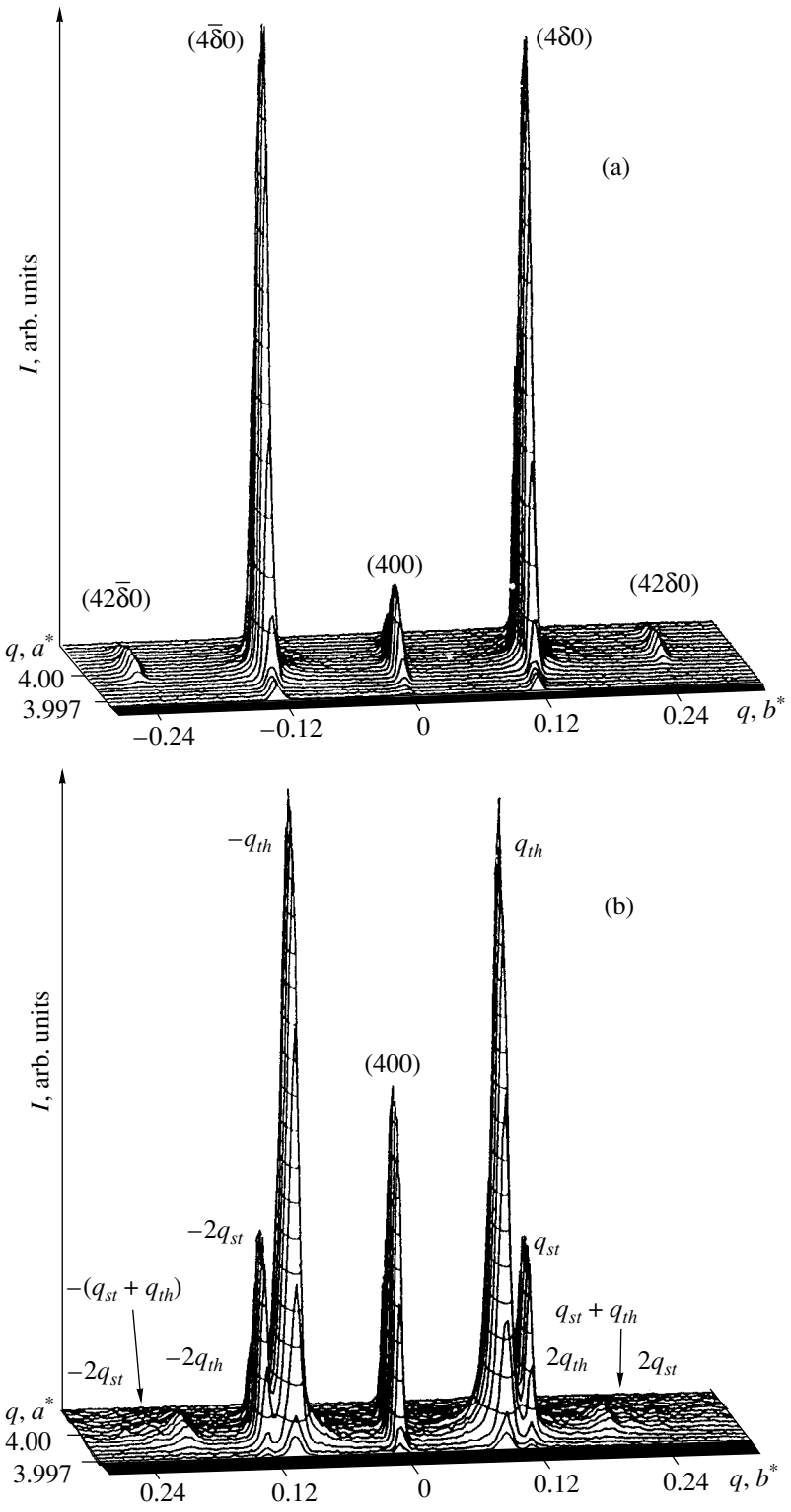

Fig. 1. Two-dimensional X-ray diffraction patterns obtained for thiourea in the reciprocal lattice region near the (400) point (a) before and (b) after 28 h-annealing at 182 K.

The X-ray diffraction was performed using the D-500 diffractometer (Siemens) modified for studying single crystals. The temperature-dependent measurements were taken in a helium cryostat designed at the Institute of Solid-State Physics of the Russian Academy of Sciences. The cryostat was supplied with a cryogenic insert allowing studies under oriented mechanical loads. The temperature and the load magni-

tude were maintained accurate to 0.1°C and 0.5 bar, respectively.

The defect density waves were observed based on the following idea. The DDW arise owing to the diffusion of defects, and this process takes quite a long time. Therefore, the periodic distribution of the defect density should survive for a certain time outside the temperature range of the incommensurate phase. However, in the incommensurate phase, the periodic distribution is the equilibrium one, while, outside this phase, the defects are out of equilibrium, and they can cause distortions of the main lattice with the period of the defect density wave. In this case, one should expect the X-ray diffraction from this periodic distortions. This effect was observed for the thiourea crystals.

Figure 1a demonstrates the region of the reciprocal lattice in the vicinity of the (400) site at 182 K (within the temperature range of the incommensurate phase). Here, we can see the satellite reflections of the first and second order in the **b*** direction. Keeping the sample at this temperature for tens of hours did not cause any appreciable changes in the intensities or the reflection profiles. However, the subsequent temperature changes gave rise to significant changes in the spectra. The same spectrum obtained at 170 K after keeping the sample at 182 K for 28 h is shown in Fig. 1b. We can see that the satellite reflections of the first order are split into two components while the Bragg reflection remains nearly unchanged. This gives an indication to the presence of at least two modulation waves in the crystal with wave vectors $\mathbf{q}_{th}$ and $\mathbf{q}_{st}$ in the **b*** direction.

The temperature dependences of the wave vectors $\mathbf{q}_{th}$ and $\mathbf{q}_{st}$ obtained by processing the spectra are shown in Fig. 2a. It is clearly seen that one wave vector ($\mathbf{q}_{st}$) remains unchanged throughout the entire range of the incommensurate phase (the stabilized wave). It coincides with the modulation wave vector at the annealing temperature, which gives an indication to the "freezing" of the initial wave in the course of annealing. The wavevector of the second wave ($\mathbf{q}_{th}$) has the usual temperature dependence similar to that observed in the crystal without annealing—Fig. 2b (the equilibrium wave). This result differs from earlier predictions, according to which the ordinary modulation wave is pinned by the defect density wave. In the latter case, we should observe a "plateau" in the temperature dependence of the modulation vector [8] rather than a newly formed additional wave. Therefore, the memory effects can be interpreted as the manifestation of the crystal transformation from the single-wave modulated state in the vicinity of the annealing temperature (corresponding to the intersection of the curves characterizing the temperature dependence of the wave vectors) to the multiwave state outside this temperature range.

The one-dimensional X-ray diffraction patterns for thiourea taken at temperatures above (205 K) and below (165 K), the temperature range of the incommensurate phase, are shown in Fig. 3. We can see that,

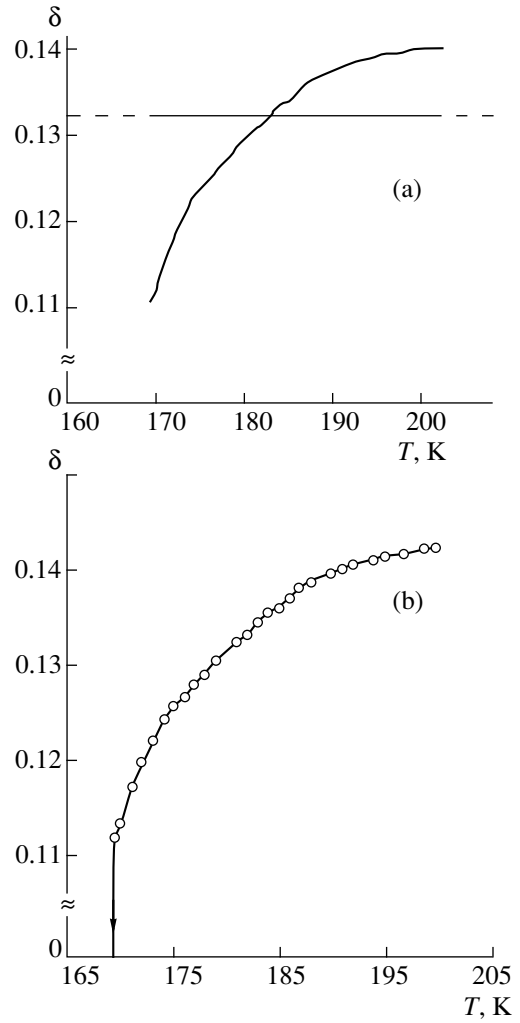

Fig. 2. Temperature behavior of the wave vectors (a) for the stabilized (straight line) and the equilibrium waves in thiourea crystal after a prolonged annealing at T = 182 K and (b) for the stabilized wave in an unannealed thiourea crystal.

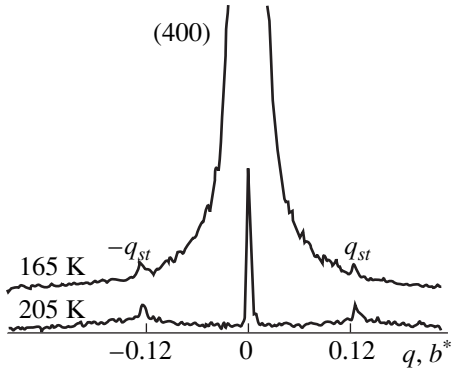

Fig. 3. Typical X-ray diffraction patterns obtained for thiourea outside the range of the incommensurate phase at 165 K (ferroelectric phase) and 205 K (paraelectric phase) after prolonged annealing at T = 182 K.

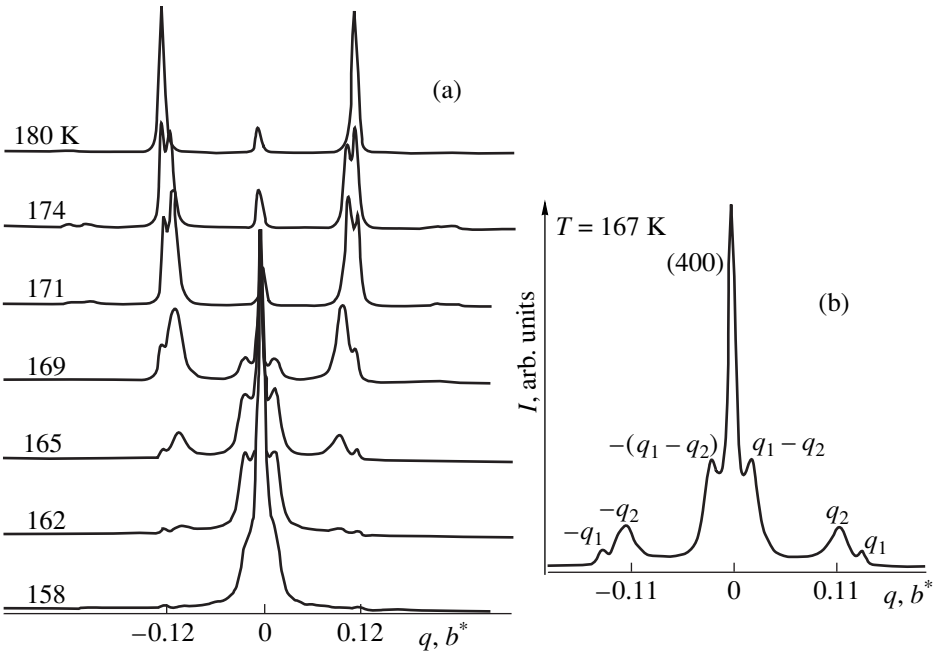

Fig. 4. (a) Temperature-dependent transformation of the X-ray diffraction patterns for thiourea after 28 h- and 7 h-annealing at 182 K and 170 K, respectively; (b) X-ray diffraction pattern of the modulated state with the superposition of two defect density waves.

in the positions corresponding to the frozen wave vector, the reflections "survive." They have much lower intensity then the satellites within the incommensurability range but their halfwidth remains the same. The narrow satellite reflections indicate that the corresponding structure modulations extend over the whole crystal as the ordinary incommensurate modulations. We suggest that the observed satellites display the X-ray diffraction from the periodic distortions of the initial lattice—the distortions caused by the nonequilibrium defects forming the defect density waves in the incommensurate phase [9].

The satellite reflections observed outside the range of the incommensurate phase (see Fig. 3) and the superstructure reflections characterizing the incommensurate phase disappear after the prolonged exposures of the sample at temperatures different from T_0. The decay time of these states is comparable with the time of the DDW formation. This suggests a common origin of the satellites observed inside and outside the incommensurate phase range and gives additional evidence of the formation of the defect density waves in the cause of the prolonged exposure of the sample at a fixed temperature within the incommensurate phase range.

The analysis of the X-ray diffraction patterns allows us to make certain conclusions concerning the structural state of the crystal in the case of the coexistence of several modulation waves after the DDW formation. Two situations are possible: (1) the crystal has a domain-type structure with the adjacent domains corresponding to the waves with different wave vectors; (2) the superposition of coexisting modulation waves extends over the whole sample volume. In the second case, the X-ray diffraction patterns should exhibit the additional satellite reflections characterized by the sum ($\mathbf{q}_{th} + \mathbf{q}_{st}$) and difference ($\mathbf{q}_{th} - \mathbf{q}_{st}$) harmonics. Such harmonics were revealed in the X-ray diffraction patterns. In Fig. 1b, the sum harmonics (indicated by arrows) are situated between the second order satellites. The difference harmonics were most clearly pronounced in the experiment when the crystal was sequentially annealed at temperatures T_{0_1} and T_{0_2}. Such annealing gave rise to the formation of two defect density waves. Figure 4 shows the temperature-dependent transformation of one-dimensional spectra for a crystal annealed at T_{0_1} = 182 K for 28 h and at T_{0_2} = 170 K for 7 h. The figure demonstrates that, as the crystal approaches the low-temperature boundary of the incommensurate phase, new symmetric satellites appear near the Bragg reflection in addition to the ordinary satellites from the defect density waves. The positions of the news satellites correspond to the difference harmonics $\mathbf{q}_{st1} - \mathbf{q}_{st2}$ (Fig. 4b).

The influence of the defect density waves on the temperature range of the incommensurate phase was revealed by annealing the samples at different temperatures within the incommensurability range. At annealings near T_i = 202 K, the temperature range of the incommensurability became wider by several degrees. At the same time, the transition point T_C = 169 K measured independently based on the temperature behavior

of the lattice constants remained unchanged. We suggest that the increase in the transition temperature between the normal and incommensurate phases only seems to be a manifestation of the phase-correlated pinning of phase fluctuations by the defect density wave. The incommensurate phase fluctuations clearly manifest themselves in the X-ray diffraction pattern corresponding to T = 205 K (Fig. 3) in the form of broad reflections with the maxima at the positions close to those related to the DDW. If the fluctuations are phase-correlated by the defect density wave, the diffracted beams are "insensitive" to unmodulated portions of the crystal, and the whole picture is similar to the reflection from the bulk crystal.

The unusual effect of defect density waves on the structural states of thiourea was revealed in the course of dynamical experiments aimed at studying the effect of continuous cooling on the temperature ranges of different phases. The experiments demonstrated that, even in the initial state of the crystal, the diffraction peaks corresponding to the basis angles of the reciprocal lattice are anomalously broadened. This broadening far exceeds the spectral broadening related to the deviation from the monochromatism in the spectral lines of the X-ray radiation in use, and it cannot be interpreted as a result of local distortions of the crystal or the block structure of the sample. It was found that, on continuous cooling at a rate of several degrees per minute, these broadened reflections were split into a series of narrow components, provided that the crystal was preliminarily annealed within the incommensurability range to form the DDW. In Fig. 5, we present the profiles of the (800) diffraction reflection before the annealing (envelope) and after the annealing at 180 K and the subsequent cooling at a rate 3 K/min ("comb"). The splitting of the initial spectrum into a large number of components suggests the formation of a long-period modulated structure with the wave vector along the **a*** direction normal to the wave vector of the ordinary modulations. The period of the "new" modulations depends on temperature and on the annealing time corresponding to the DDW generation (on the wavelength of DDW). Note that, after the annealing of the sample characterized by the decay of the defect density wave, the broad lineshape is restored.

The selection of some components of the long-wavelength modulations by the defect density waves can be related to the fact that the efficient pinning is possible only for the modulations that are phase-correlated with DDW. In this case, the change in the DDW wavelength and its profile will cause a change in the frequency of the wave responsible for the pinning, which leads to the dependence of the period of the long-wavelength modulations on temperature and on the annealing time.

The long-wavelength modulations of the structure were also found in other compounds with the incommensurally modulated phases. Figure 6 demonstrates

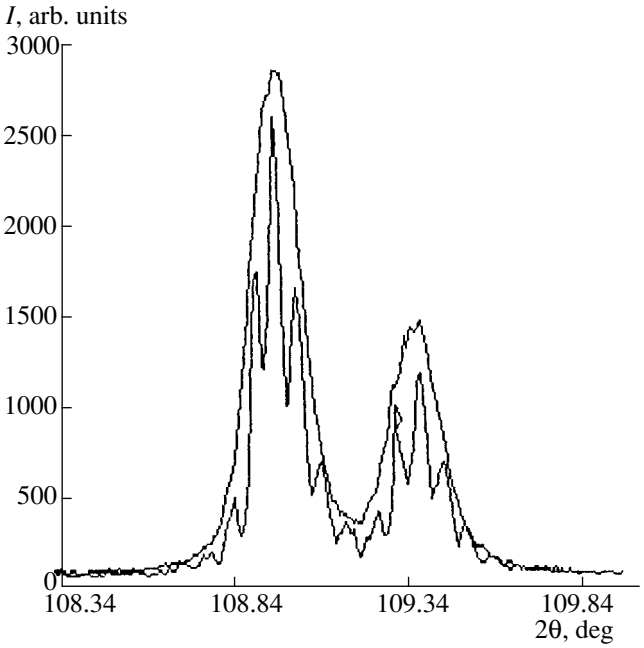

Fig. 5. Profiles of the (800) reflection from thiourea before (envelope) and after annealing at 182 K and subsequent constant-rate cooling (inner curve).

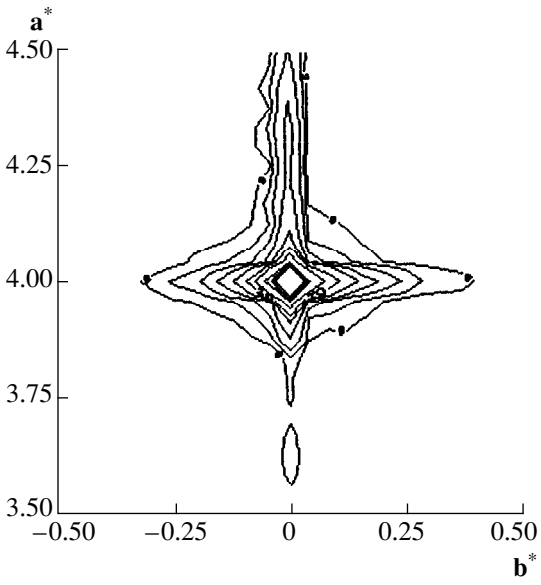

Fig. 6. Two-dimensional pattern of the (400) reflection in the **a***–**b*** plane for Rb_2ZnCl_4 at room temperature.

the section of the (400) reciprocal lattice site by the **a***–**b*** plane for Rb_2ZnCl_4 at room temperature. We can see that this peak is continuously broadened both in **a*** and **b*** directions. The extension of the peak in the **a*** direction is a consequence of using a nonmonochromatic X-ray spectrum. The spectral components along **b*** can be interpreted as a continuous (in frequency) set of structure modulations with small wave vectors. In con-

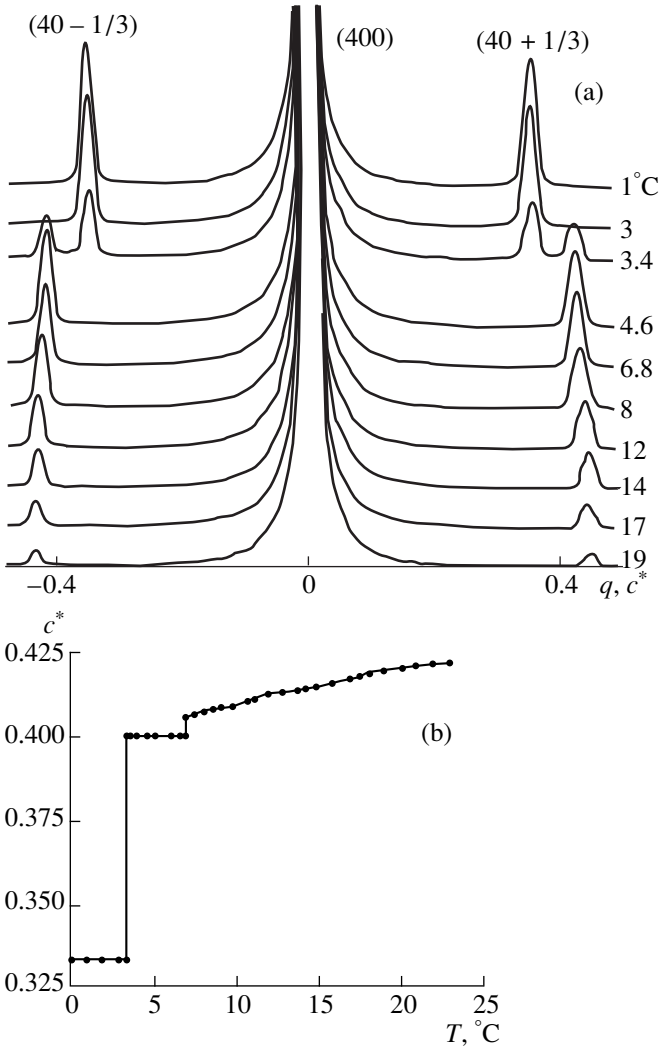

Fig. 7. (a) Temperature-dependent transformation of the X-ray diffraction patterns for TMA-$ZnCl_4$ in the range of existence of the modulated phase (atmospheric pressure); (b) temperature variations of the wave vector in TMA–$ZnCl_4$ under the atmospheric pressure.

trast to thiourea, the vectors of the long-wavelength modulations in Rb_2ZnCl_4 are directed along the wave vector of the ordinary incommensurate modulation. We also note that the long-wavelength structure modulations are observed not only in the incommensurate phase range but in the normal phase as well. The nature of these modulations is still unclear. Further studies are needed to reveal the conditions of formation of such modulations, their temperature range of existence, their spectral composition, and the temperature dependence of their wave vectors.

The unexpected effect of the defect density waves on the structural states of crystals with incommensurate phases was revealed by studying the σ_{yy}–T phase diagram of TMA–$ZnCl_4$ crystals. As it was mentioned earlier, small stresses "remove" the polar phase in these crystals. In our experiments, we used the oriented mechanical loads along the b axis. We analyzed the X-ray diffraction patterns in the **a***–**c*** plane of the reciprocal lattice. The temperature-induced transformation of the X-ray diffraction patterns at the atmospheric pressure is shown in Fig. 7a. The corresponding temperature behavior of the modulation wave vectors is illustrated in Fig 7b. The σ_{yy}–T phase diagram deduced from these patterns is shown in Fig. 8. We can see that the polar phase characterized by the wave vector $\mathbf{q} = 2/5\mathbf{c}^*$ disappears at critical stresses σ_{yy} about 40 bar.

The transitions between the incommensurate and polar phases and between the polar and ferroelastic phases are the first order transitions. This fact was confirmed experimentally by the appearance of two-phase states near the phase boundaries in the phase diagram. In the case of appreciable loads applied to the crystal (>15 bar) with the polar phase range being significantly narrowed, three phases coexisted simultaneously.

The X-ray diffraction pattern of TMA–$ZnCl_4$ loaded with 10 bar at 6.7°C is shown in Fig 9a. It corresponds to the two-phase state combining the incommensurate and polar phases. In addition to the satellite reflections $\mathbf{q}_1$ of the incommensurate phase and $\mathbf{q}_2$ of the polar phase, the pattern exhibits the difference harmonics $\mathbf{q}_1 - \mathbf{q}_2$ giving clear indications to the superposition of these phases [10]. In contrast to thiourea, where the superposition of two incommensurate phases takes place, in TMA–ZnCl, the superposition of the two neighboring phases was observed. If the two-phase state is formed by the polar and ferroeleastic phases, then two situations take place. Under uniaxial stresses in the absence of the three-phase state (low stresses), the superposition is not observed. If the ferroelastic phase initially coexisted with the polar and incommensurate phases, the superposition of the polar and ferroelastic phases takes place. The X-ray diffraction pattern corresponding to such a superposition at $\sigma = 15$ bar and $T = 4.2$°C is shown in Fig. 9b.

The crystal state characterized by the superposition of phases cannot be referred to as a two-phase state. In the ordinary two-phase state, the crystal is subdivided into the portions (domains) of different phases. In the case of superposition, both modulations extend over the whole volume. In our opinion, it is more correct to consider this situation as a mixed state. Its formation is stimulated by the defect density waves causing modulated distortions of the lattice and subsequent correlations of the arising modulations with this distortion field.

The characteristic effect of the defect density waves on the kinetics of the transition between the normal and incommensurate phases was observed for proustite crystals [11]. The temperature dependence of the intensity of the (–606) reflection is shown in Fig. 10a for the temperature range including the transition between the normal and incommensurate phases. The arrows indicate the direction of temperature changes in the heat-

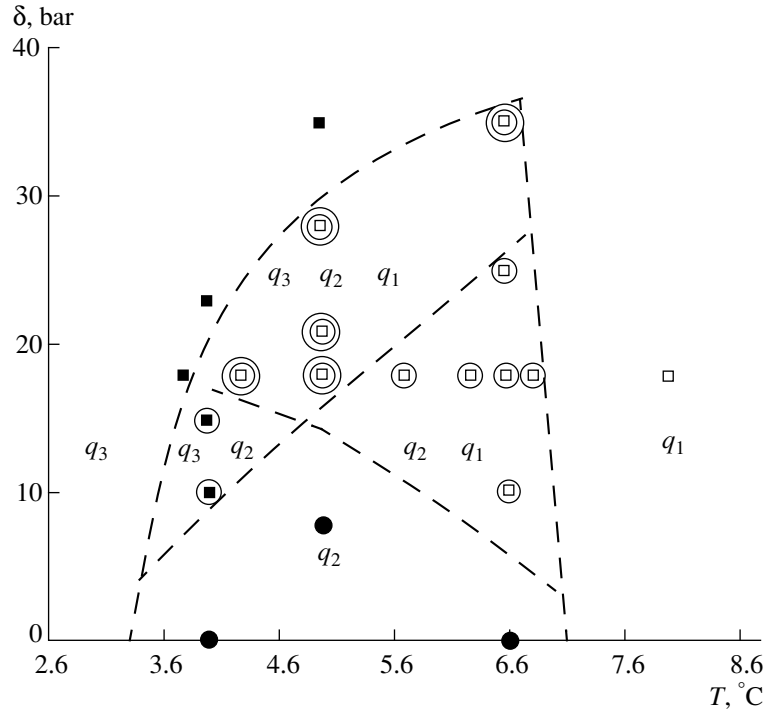

Fig. 8. Phase diagram in the σ_{yy}–T plane for TMA–$ZnCl_4$ (dashed lines show the boundaries of two- and three-phase regions).

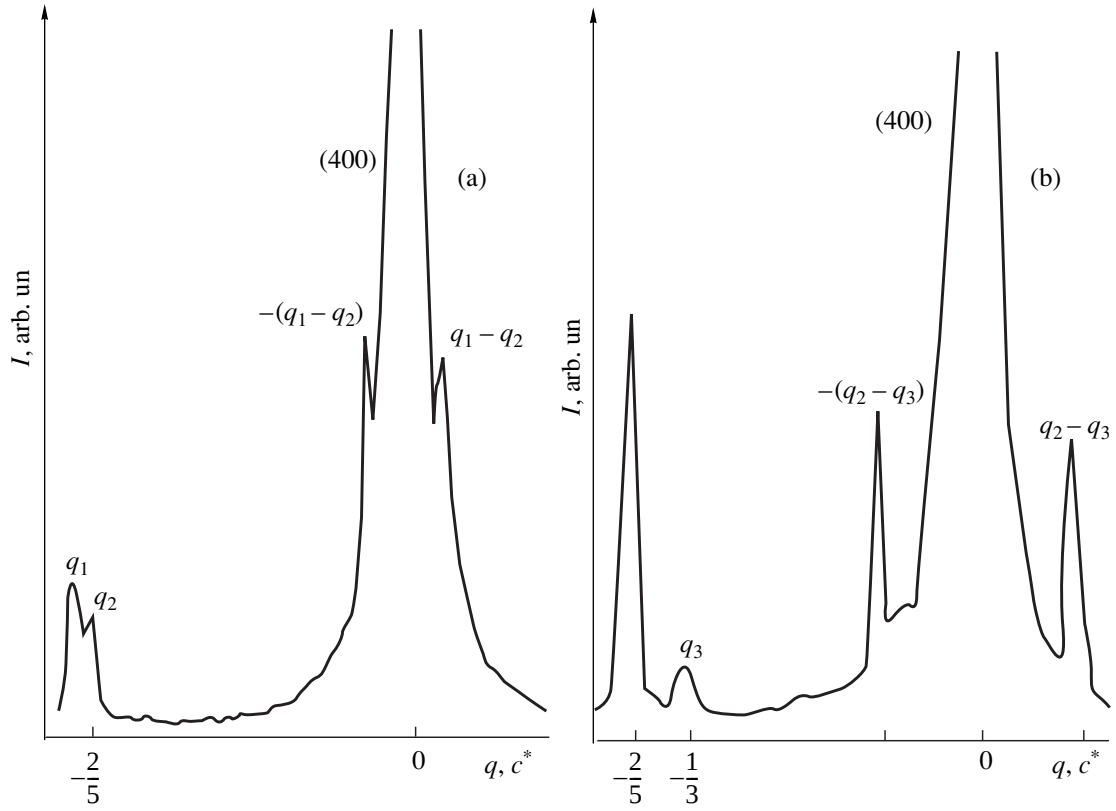

Fig. 9. X-ray diffraction patterns corresponding to the mixed states in TMA–$ZnCl_4$: (a) incommensurate and polar phases, (b) polar and ferroelectric phases.

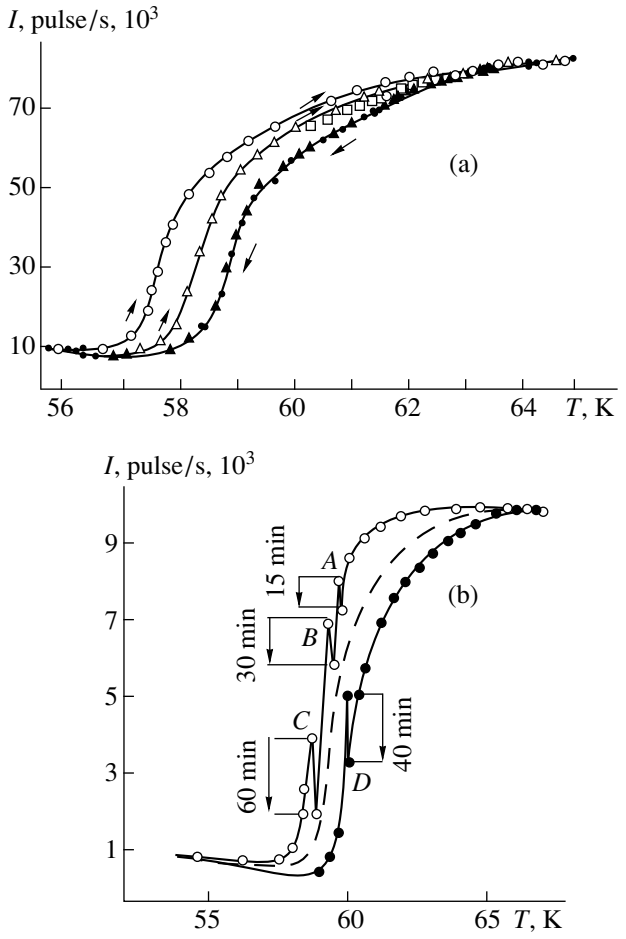

Fig. 10. Temperature-dependent intensity variations for the (–606) Bragg reflection in proustite near the transition between the normal and the incommensurate phases: (a) dependence of the transition hysteresis on the initial temperature in the reverse cycle (at each temperature point, the sample was kept for 3 min); (b) relaxation variations of diffraction intensity during prolonged cooling (point D) and heating (points *A*, *B*, and *C*) of the crystal. The dashed curve shows possible intensity variations during infinitely slow cooling.

ing–cooling cycles. The experiment revealed the hysteretic behavior if the intensity variations. From the theoretical viewpoint, the transition between the normal and incommensurate phases is of the second order, i. e., without any hysteresis. In the actual crystal, it turns out to be the first order phase transition due to the finite temperature variation rate and the presence of lattice defects (see Fig. 10). In this case, we observe the unusual reverse hysteresis with the transition temperature being higher on cooling than on heating. The lower is the temperature the wider is the hysteresis loop. We propose the following model of this phenomenon. The transition of the crystal to the incommensurate phase is accompanied by the formation of the defect density wave. As the temperature is lowered, the wavelength corresponding to the ordinary structure modulation varies and causes the displacement of the defect density wave owing to both the diffusion of defects and their generation at the new positions. These changes are accompanied by the interaction between the incommensurate phase and the DDW. Such interaction should depend on the elastic properties of the modulation lattice, on the rate of change of the period of this lattice (on the rate of the temperature variation in the sample), and on the diffusion rate of the point defects forming the DDW. On cooling (heating), the situation depends on whether the rearrangement of the defect density wave will be quick enough to follow the variations of the period of the incommensurate structure. If not, then, beginning from a certain temperature, the DDW will act as a pinning center impeding the temperature variation of the modulation lattice period, and, finally, at some other temperature, the modulation lattice will be destroyed. It is clear that the destruction is most probable in the vicinity of the phase transition where the incommensurate structure is loosened. It is also clear that the lower is the temperature of the reverse cycle the larger is the difference between the wavelength of the DDW formed at this temperature and the modulation lattice period near the transition between the incommensurate and the normal phases, which means that, at lower temperatures, the destruction of the modulation lattice will occur earlier.

In such a model, we should expect certain relaxation phenomena to occur during the crystal exposure within the temperature range corresponding to the hysteresis. These phenomena reflect tuning of the defect density wave to the modulation wave of the structure. In Fig. 10b, such relaxation manifests itself in the intensity variations of the basic reflection depending on the temperatures of the preliminary sample exposure. It is clear that in the limit of an infinitely long sample exposure at each temperature point, the hysteresis will be absent, and the transition between the normal and incommensurate phases will be of the second order.

In conclusion, we note that the above-listed specific effects related to the defect density waves do not always occur in a complete form in every crystal with incommensurate modulations of their structure. In our opinion, this fact can be explained by the differences in the defect types, their activation energy and diffusion mobility, as well as by the difference in the structure modulations characteristic of different crystals.

ACKNOWLEDGMENTS

This work was supported in part by the Russian Foundation for Basic Research (project no 94-02-04826) and by INTAS (grant no. 93-3230).

REFERENCES

1. Hamano, K., Ema, K., and Hirotsu, S., *Ferroelectrics*, 1981, vol. 36, p. 343.

2. Jamet, J.P. and Lederer, P.J., *Phys. Lett. A*, 1983, vol. 44, p. 257.
3. Vikhnin, V.S., *Trudy Mezhdunarodnogo simpoziuma "Sinergetika i kooperativnye yavleniya v tverdykh telakh i makromolekulakh"* (Proc. Int. Simp. "Synergetics and Cooperative Phenomena in Solid States and Macromolecules"), Tallin: Vilgus, 1983, p. 91.
4. Vikhnin, V.S., *Dielektriki i poluprovodniki* (Insulators and Semiconductors), Kiev: Vysshaya Shkola, 1983, no. 24, p. 3.
5. Lederer, P.J., Montambaux, G., Jamet, J.P., and Chauvin, M., *Phys. Lett. A*, 1984, vol. 45, p. 627.
6. Vikhnin, V.S., *Izv. Akad. Nauk SSSR, Ser. Fiz.*, 1986, vol. 50, no. 2, p. 340.
7. Khasanov, S.S., Shekhtman, V.Sh., and Shmyt'ko, I.M., *Fiz. Tverd. Tela* (Leningrad), 1984, vol. 26, p. 935.
8. Jamet, J.P., *Phase Transitions*, 1988, vol. 11, p. 335.
9. Bagautdinov, B.Sh. and Shmyt'ko, I.M., *Pis'ma Zh. Eksp. Teor. Fiz.*, 1994, vol. 59, no. 3, p. 171.
10. Bagautdinov, B.Sh., Gladkii, V.V., Kallaev, S.N., *et al.*, *Pis'ma Zh. Eksp. Teor. Fiz.*, 1994, vol. 59, no. 2, p. 113.
11. Shmyt'ko, I.M., Shekhtman, V.Sh., Bagautdinov, B.Sh., and Afonikova, N.S., *Fiz. Tverd. Tela* (Leningrad), 1990, vol. 32, p. 2441.

Translated by K. Kugel